

# FE-Simulation of Fast Switching Behavior of Granular Nanoelements

J. Fidler, T. Schrefl, V. D. Tsiantos, H. Forster, R. Dittrich, and D. Suess

**Abstract**—Transient magnetization states during switching are investigated numerically in thin granular square shaped nanoelements ( $100 \times 100 \text{ nm}^2$ ) with uniaxial (Co-hcp), cubic anisotropy (Co-fcc) and zero anisotropy ( $\text{Ni}_{80}\text{Fe}_{20}$ ) with 10 nm grain size and a thickness of 10 nm and taking into account a random orientation of the grains using a hybrid finite-element/boundary-element model. In-plane switching dynamics are calculated for external fields with a constant sweep rate of 0.02 and  $2.0J_s/(\mu_0 \cdot \text{ns})$ . The switching time and critical field strongly depends on the Gilbert damping parameter and sweep rate. Largest switching times and fields were found for the Co thin film element with uniaxial anisotropy, such as 5 ns and 120 kA/m for  $0.02J_s/(\mu_0 \cdot \text{ns})$  and 0.1 ns and 245 kA/m ( $\alpha = 0.02$ ) and 329 kA/m ( $\alpha = 1.0$ ) for  $2J_s/(\mu_0 \cdot \text{ns})$ , respectively. Depending on the sweep rate the fastest in-plane switching occurs in the granular cubic Co- and permalloy-thin film elements ( $<2 \text{ ns}$  for  $0.02J_s/(\mu_0 \cdot \text{ns})$  and  $0.1 \text{ ns}$  for  $2J_s/(\mu_0 \cdot \text{ns})$ ). The smallest switching fields are obtained in NiFe with zero anisotropy, i.e.,  $<20 \text{ kA/m}$  for  $0.02J_s/(\mu_0 \cdot \text{ns})$  and  $<140 \text{ kA/m}$  for  $2J_s/(\mu_0 \cdot \text{ns})$ . Precessional oscillation effects occurred in the ( $\text{Ni}_{80}\text{Fe}_{20}$ ) square element for a small damping constant ( $\alpha = 0.02$ ). The transient magnetization states during reversal vary from nucleation and expansion of reversed domains (Co-hcp) to inhomogeneous rotation inside the nanoelements with cubic (Co-fcc) and zero anisotropy ( $\text{Ni}_{80}\text{Fe}_{20}$ ).

**Index Terms**—Co nanoelements, NiFe nanoelements, numerical micromagnetics, precessional switching.

## I. INTRODUCTION

**B**RILLOUIN light scattering, *in situ* domain observation using Lorentz electron microscopy, magnetic force microscopy, and time-resolved magnetic imaging provides a detailed understanding of the spin wave modes [1], domain formation and reversal processes occurring in mesoscopic and nanoscopic structured magnetic elements [2]. Numerical micromagnetics based on the Landau–Lifshitz–Gilbert equation of motion gives the information about the magnetization switching processes. Experimental and numerical studies have shown that the switching fields and times which are in the order of ps to ns are controlled by the choice of the geometric shape, size and microstructure of the nanomagnets, the intrinsic properties and the orientation and strength of the applied field and considerably depend on the damping constant [3]–[8]. With decreasing size of the magnetic structures, thermally activated reversal process becomes significant, if switching times are larger than approximately 0.5 ns [8]. In this paper, the reversal process within granular nanoscale squares are performed to examine the influence of magnetocrystalline anisotropy on the

Manuscript received February 12, 2002. This work was supported by the Austrian Science Fund under Grant P13260-TEC and Grant Y-132 PHY.

The authors are with Solid State Physics, Vienna University of Technology, A-1040 Wien, Austria (e-mail: fidler@tuwien.ac.at).

Digital Object Identifier 10.1109/TMAG.2002.801910.

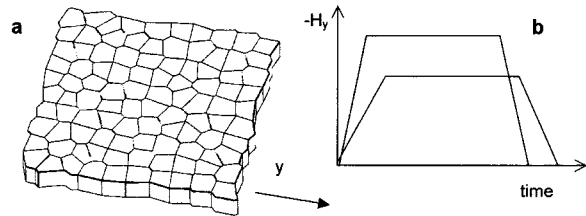


Fig. 1. (a) Schematic geometry of granular structure of a square thin film element with the dimensions of  $100 \times 100 \times 10 \text{ nm}^3$  consisting of 100 grains with a grain size of about 10 nm. (b) Different magnetic field profiles with different sweep rates and constant field values ( $H = H_c$ ) of the applied field along to the  $-y$  direction were used for the numerical simulations.

switching behavior of thin Co and permalloy film elements. Thermal fluctuations, defects and other forms of disorder as well as eddy currents are not included in the simulations. Due to the small size eddy currents occurring during the fast switching process are considered to be small and therefore are neglected.

## II. MICROMAGNETIC MODEL

We have used a three-dimensional (3-D) numerical micromagnetic model with tetrahedral finite elements with a constant edge length of 2–5 nm to study thin (10 nm) square-shaped structures with an edge length of about 100 nm comparing the influence of material parameters (Co-hcp, Co-fcc and  $\text{Ni}_{80}\text{Fe}_{20}$ ) on the switching behavior. The nanoelement consists of randomly orientation grains of about 10 nm. The granular thin film element is modeled with columnar grains generated from Voronoi polyhedrons. The basic geometry of the granular thin film element is shown in Fig. 1(a). For the simulations we used three sets of materials parameters: The  $\text{Ni}_{80}\text{Fe}_{20}$  nanoelement has the following material properties:  $J_s = 1 \text{ T}$ ,  $K_1 = K_2 = 0$ , and  $A = 13 \text{ pJ/m}$ . The polycrystalline Co square element consists whether three dimensionally, randomly oriented grains with uniaxial anisotropy (Co-hcp:  $J_s = 1.76 \text{ T}$ ,  $K_1 = 0.45 \text{ MJ/m}^3$ ,  $K_2 = 0.15 \text{ MJ/m}^3$ ,  $A = 13 \text{ pJ/m}$ ) or cubic anisotropy (Co-fcc [9]:  $J_s = 1.76 \text{ T}$ ,  $K_1 = 0.05 \text{ MJ/m}^3$ ,  $K_2 = 0$ ,  $A = 13 \text{ pJ/m}$ ). The micromagnetic method combines a hybrid finite element/boundary element method for the magnetostatic field calculation with a BDF/GMRES method for the time integration [10].

The time evolution of the magnetization at each nodal point of the finite element mesh was calculated using the Gilbert equation. Different external field profiles [Fig. 1(b)] were used for the simulations. In the first stage, a monotone increasing “sweep” field with constant sweep rate (0.02 to  $2.0J_s/\mu_0$  per ns) was uniformly applied along the  $-y$  direction until complete magnetization reversal took place. Second, a

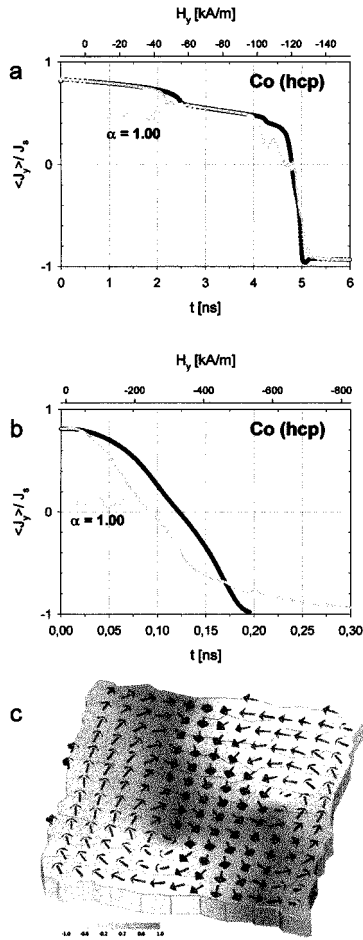


Fig. 2. Time evolution of the polarization inside the granular uniaxial Co-hcp square element during the application of a unidirectional field with a sweep rate of (a)  $0.02 J_s / (\mu_0 \cdot \text{ns})$  or  $28 \text{ kA} / (\text{m} \cdot \text{ns})$ , (b)  $2.0 J_s / (\mu_0 \cdot \text{ns})$  or  $2800 \text{ kA} / (\text{m} \cdot \text{ns})$ , and (c) showing the transient magnetization state at  $H = H_c$  for  $\alpha = 0.02$  and  $0.02 J_s / (\mu_0 \cdot \text{ns})$ .

homogeneous, constant field was applied after rising the field to  $H = H_c$ .

### III. RESULTS AND DISCUSSION

The switching behavior and switching times were found to differ for randomly oriented, uniaxial Co-grains (hcp), Co-grains with cubic anisotropy (fcc) and NiFe nanoelements with zero anisotropy. Fig. 2(a) and (b) compare the time evolution of the polarization of uniaxial Co-grains (hcp) for different damping constants and field rise times starting from the remanent state of magnetization. For a slow sweep rate of  $0.02 J_s / (\mu_0 \cdot \text{ns})$  the switching occurs only after a waiting time of about 5 ns independently of the damping parameter [Fig. 2(a)]. For small external field values, the Zeeman energy contribution is not sufficient to overcome the large dipolar and anisotropy energies and, therefore, leading to relatively large switching times. The switching time reduces to about 0.1 ns for  $\alpha = 0.02$  for a high sweep rate value of  $2 J_s / (\mu_0 \cdot \text{ns})$  [Fig. 2(a)]. As a result of the simulations, switching ( $\langle J_y \rangle = 0$ ) occurs at different switching fields  $H_{\text{sw}}$  for low and high sweep rates. For  $0.02 J_s / (\mu_0 \cdot \text{ns})$   $H_{\text{sw}} = 120 \text{ kA/m}$  for both,  $\alpha = 0.02$  and  $1.00$ , whereas faster switching is observed for

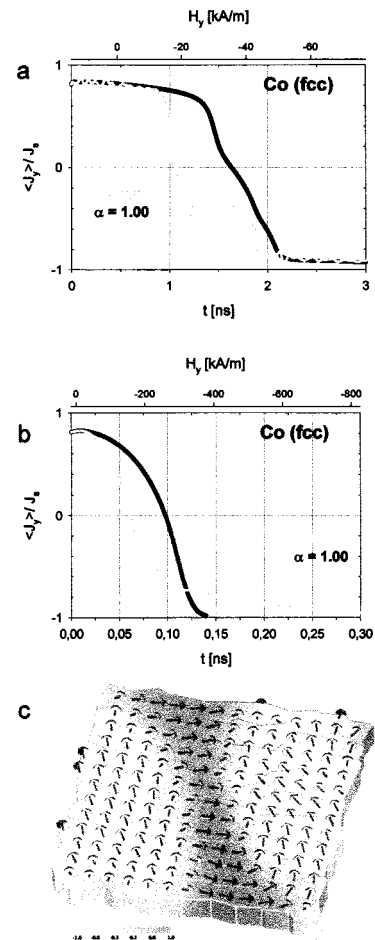


Fig. 3. Time evolution of the polarization inside the granular cubic Co-fcc square element during the application of a unidirectional field with a sweep rate of (a)  $0.02 J_s / (\mu_0 \cdot \text{ns})$  or  $28 \text{ kA} / (\text{m} \cdot \text{ns})$ , (b)  $2.0 J_s / (\mu_0 \cdot \text{ns})$  or  $2800 \text{ kA} / (\text{m} \cdot \text{ns})$ , and (c) showing the transient magnetization state at  $H = H_c$  for  $\alpha = 0.02$  and  $2 J_s / (\mu_0 \cdot \text{ns})$ .

lower damping rate,  $H_{\text{sw}} = 245 \text{ kA/m}$  for  $\alpha = 0.02$  and  $H_{\text{sw}} = 329 \text{ kA/m}$  for  $\alpha = 1.00$ . Differences in minimum switching times depending on the damping parameter were also found in [4] investigating the reversal times of a single domain ultra-thin film. The simulations show that for the Co-hcp thin film the magnetization reversal mechanisms are similar for low and high damping parameters and low and high sweep rates. The typical transient magnetization states, such as shown in Fig. 2(c) for  $0.02 J_s / (\mu_0 \cdot \text{ns})$  and  $\alpha = 0.02$  at  $\langle J_y \rangle = 0$ , indicate that nucleation and magnetization reversal primarily occurs at opposite corners of the nanoelement. Inhomogeneous magnetization rotation processes are dominant and lead the expansion of the reversed domains.

In the case of randomly oriented grains with cubic anisotropy, the simulations show a decrease of the switching time and field, which depend again on the sweep rate and the damping constant  $\alpha$ , are reduced to values less than 2.0 ns or less than 40 kA/m [Fig. 3(a)] for the low sweep rate of  $0.02 J_s / (\mu_0 \cdot \text{ns})$  and less than 0.1 ns or 230 kA/m for  $2 J_s / (\mu_0 \cdot \text{ns})$  [Fig. 3(a)]. The magnetization reversal processes during switching ( $\langle J_y \rangle = 0$ ) are different for randomly oriented Co-fcc grains from the case of uniaxial Co grains. The numerical micromagnetic simulations reveal rotational magnetization reversal inside the gran-

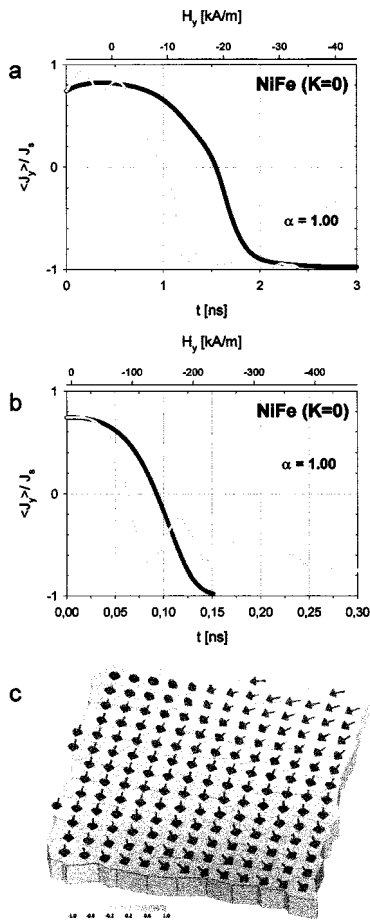


Fig. 4. Time evolution of the polarization inside the  $\text{Ni}_{80}\text{Fe}_{20}$  square element with  $K = 0$  during the application of a unidirectional field with a sweep rate of (a)  $0.02 J_s / (\mu_0 \cdot \text{ns})$  or  $16 \text{ kA} / (\text{m} \cdot \text{ns})$ , (b)  $2.0 J_s / (\mu_0 \cdot \text{ns})$  or  $1600 \text{ kA} / (\text{m} \cdot \text{ns})$ , and (c) showing the transient magnetization state at  $H = H_c$  for  $\alpha = 0.02$  and  $0.02 J_s / (\mu_0 \cdot \text{ns})$ .

ular nanoelement starting from the end domains perpendicular to the field direction. The kind of the inhomogeneous rotation is similar for  $\alpha = 0.02$  and  $1.00$ . The magnetization pattern of Fig. 3(c) show the magnetization distribution for  $\alpha = 0.02$  and for the sweep rates  $2 J_s / (\mu_0 \cdot \text{ns})$ .

In the NiFe film element with  $K = 0$ , the reversal starts from the remanent state by rotating the magnetization in the end domains within the elements during the rise time, if the field is applied uniformly. The out-of-plane components are clearly observed in the magnetization pattern of Fig. 4(c) which shows

the magnetization state at  $\langle J_y \rangle = 0$  for  $\alpha = 0.02$  and a sweep rate of  $0.02 J_s / (\mu_0 \cdot \text{ns})$ . The reversal starts in the center of the element, whereas the magnetization in the regions along the square edges parallel to the field only rotated slightly. Fig. 4(a) and (b) compare the time evolution of the polarization for the different sweep rates  $H(t)$ . Compared to the switching times and fields of the granular, cubic Co (fcc) film the switching times of the NiFe film are in the same order of less than  $2 \text{ ns}$  ( $0.02 J_s / (\mu_0 \cdot \text{ns})$ ) and  $0.1 \text{ ns}$  ( $2 J_s / (\mu_0 \cdot \text{ns})$ ), whereas the critical switching fields are much lower, i.e., less than  $20 \text{ kA/m}$  [Fig. 4(a)] for the low sweep rate  $0.02 J_s / (\mu_0 \cdot \text{ns})$  and less than  $140 \text{ kA/m}$  [Fig. 4(b)] for  $2 J_s / (\mu_0 \cdot \text{ns})$ , respectively. Differently to all previous cases it is obvious that the ringing effects or the precessional oscillation of the polarization are strongly pronounced for small damping parameter ( $\alpha = 0.02$ ). Despite shorter switching time obtained for a high sweep rate the precessional instability hinders the  $\text{Ni}_{80}\text{Fe}_{20}$  nanoelement from a clear switching behavior [Fig. 4(b)]. The simulations show that an increase of the damping parameter [11], such as by doping of NiFe with heavy rare earth elements, suppresses the precessional oscillation or ringing effects resulting in short switching times and fields.

## REFERENCES

- [1] J. Jorzick, S. O. Demokritov, C. Mathieu, B. Hillebrands, B. Bartenlian, C. Chappert, F. Rousseaux, and A. N. Slavin, *Phys. Rev.*, vol. B 60, pp. 15194–15200, 1999.
- [2] S. Y. Chou, "Patterned magnetic nanostructures and quantized magnetic disks," *Proc. IEEE*, vol. 85, pp. 652–671, Apr. 1997.
- [3] W. Wernsdorfer, E. Bonet Orozco, B. Barbara, K. Hasselbach, A. Benoit, D. Mailly, B. Doudin, J. Meier, J. E. Wegrowe, J.-Ph. Ansermet, N. Demoncy, H. Pascard, A. Loiseau, L. Francois, N. Duxin, and M. P. Pileni, *J. Appl. Phys.*, vol. 81, pp. 5543–5545, 1997.
- [4] R. Kikuchi, *J. Appl. Phys.*, vol. 27, pp. 1352–1357, 1956.
- [5] T. Leineweber and H. Kronmüller, *J. Magn. Magn. Mater.*, vol. 192, pp. 575–590, 1999.
- [6] R. H. Koch, J. G. Deak, D. W. Abraham, P. L. Trouilloud, R. A. Altman, Y. Lu, W. J. Gallagher, R. E. Scheuerlein, K. P. Roche, and S. S. P. Parkin, *Phys. Rev. Lett.*, vol. 81, pp. 4512–4515, 1998.
- [7] G. Albuquerque, J. Miltat, and A. Thiaville, *J. Appl. Phys.*, vol. 89, pp. 6719–6721, 2001.
- [8] J. Fidler, T. Schrefl, V. D. Tsiantos, W. Scholz, and D. Suess, *J. Comput. Mat. Sci.*, vol. 24, pp. 163–174, 2002.
- [9] L. Holloway and H. Laidler, *IEEE Trans. Magn.*, vol. 37, pp. 1459–1461, July 2001.
- [10] J. Fidler and T. Schrefl, *J. Phys. D: Appl. Phys.*, vol. 33, pp. R135–R156, 2000.
- [11] W. Bailey, P. Kabos, F. Mancoff, and S. Russek, *IEEE Trans. Magn.*, vol. 37, pp. 1749–1754, July 2001.